GA Report

Robust Digital Position Control of a DC Servo System

Prepared by:
Heinrich Crous (CRSHEI004)
Group 2

Prepared for:
EEE4118F
Department of Electrical Engineering
University of Cape Town

May 2, 2025

0.1 Purpose of the Project

The aim of this project is to design, simulate, and implement a robust digital control system for a DC servo motor. The system must meet specific performance targets — including fast response time, low overshoot, and zero steady-state error — and continue to perform reliably even when the motor's physical properties change (e.g., variation due to added mass, braking or a change in amplifier gain).

The project is split into two main components:

- **System Identification:** Using a combination of step tests and manually applied input signals (step, ramp, and sinusoidal inputs), a mathematical model of the servo motor is developed to reflect how it behaves under different physical conditions.
- **Digital Control Design:** A cascaded controller is created, with an inner loop that manages motor speed and an outer loop that controls position. The design must work effectively across a range of plant uncertainties.

The following table summarises the key performance specifications the controller was designed to meet:

Table 1: Controller Design Specifications

Requirement	**Target Value**
Settling time ($t_{2\%}$)	< 1 second
Overshoot (OS)	$< 20\%$ (target: 10%)
Steady-state error	Zero (to step input)
Disturbance rejection	Recovery < 1 second
Robustness to plant variation	Stable under added mass and brake
Sampling time	0.05 seconds

This project provides a hands-on opportunity to apply core engineering concepts — including modelling, simulation, and real-time control — in a way that aligns with the requirements of Exit Level Outcome 2. It bridges theory and practice using MATLAB, Simulink, and laboratory testing.

0.2 System Identification and Modelling

1. Objective and Engineering Relevance

This section focuses on developing a mathematical model of the servo system based on both theory and measured data. The model is essential for designing a controller that performs well in practice, and it illustrates the application of scientific and engineering knowledge — in line with Graduate Attribute 2.

2. Experimental Setup

The system under test consists of a DC motor with feedback from a tachometer (velocity) and a potentiometer (position). Input signals were applied manually, and outputs were recorded using an oscilloscope. Three test cases were used: the nominal setup, with added brake, and with added mass.

The velocity and position outputs were recorded in volts. While these signals represent physical quantities (speed and angular displacement), they are not scaled to standard SI units — instead, they are treated as proportional indicators, consistent across all tests and sufficient for system modelling and control design.

3. Ramp Response and Deadband Identification

A slow ramp input was used to identify the motor's deadband — the range of input where no motion occurs. Once the linear operating region (between 4V and 5V) was identified, all further modelling was based on inputs in this range. The linear region was between 4V and 5V.

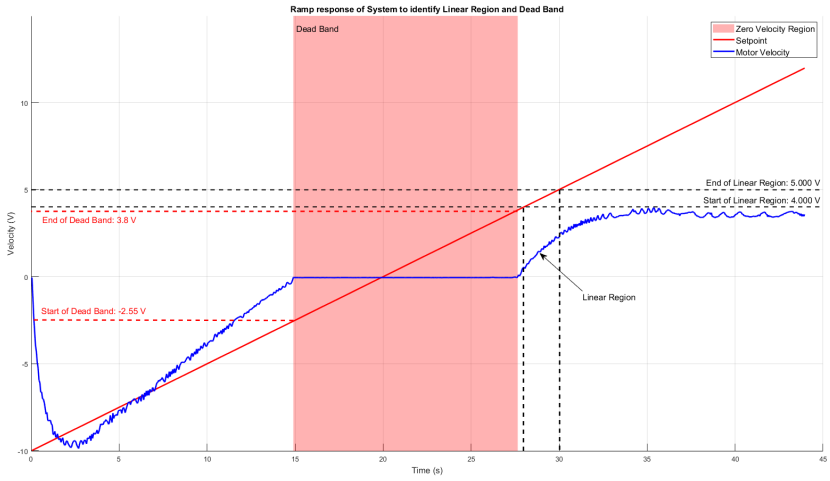

Figure 1: Ramp input response used to identify deadband and linear operating region of plant

4. Step Response Analysis

A step input was applied in the linear region. The resulting velocity response had no oscillations and rose smoothly to a steady value — a shape characteristic of first-order behaviour. This justified modelling the velocity dynamics as a first-order system, which is typical for DC motors where mechanical effects dominate and electrical dynamics settle quickly. The simplicity of a first-order model made it easy to estimate key parameters and provided a good match to the measured response, making it a solid foundation for controller design. The model took the form:

$$P_2(w) = \frac{A}{Tw + 1}$$

The gain A and time constant T were extracted directly from the step response, using the steady-state value and the time taken to reach 63.2% of that value. These parameters are shown and annotated in the corresponding figures for each case — nominal, with added brake, and with added mass — where the step responses clearly illustrate the differences in plant dynamics under each condition.

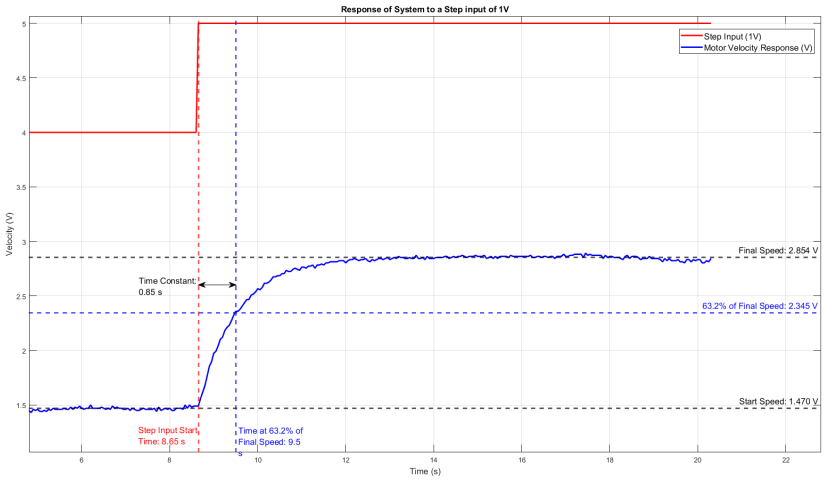

Figure 2: Measured step response for nominal case: $A = 1.384$, $T = 0.85$ s

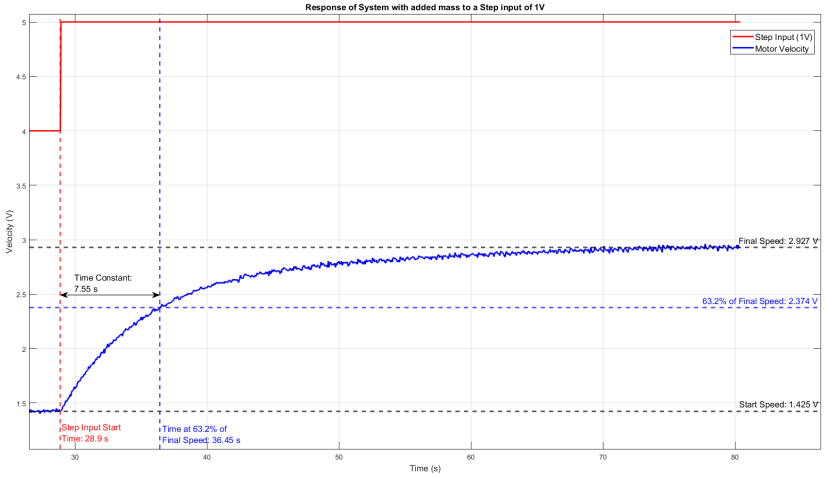

Figure 3: Measured step response for added mass case: $A = 0.437$, $T = 0.25$ s

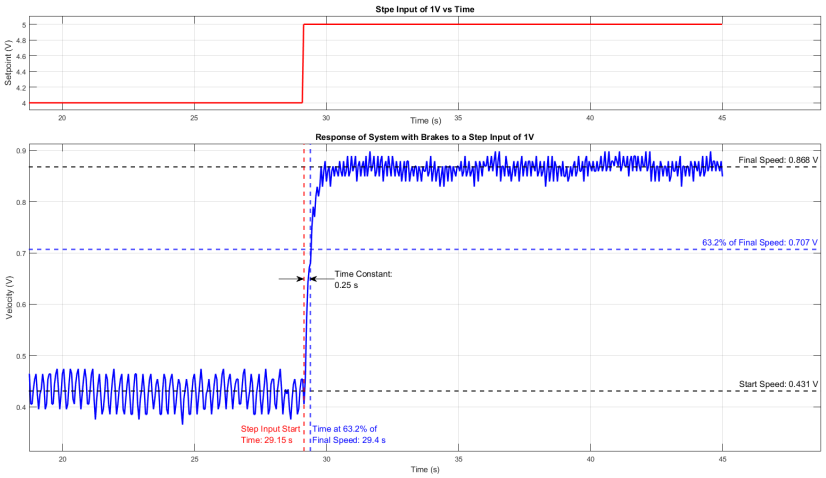

Figure 4: Measured step response for braking case: $A = 1.502$, $T = 7.555$ s

5. Position Integrator Gain Estimation

To model position, the velocity output was passed through an integrator:

$$P_1(w) = \frac{a}{w}$$

The gain a was calculated from the slope of the position ramp relative to the steady-state velocity. When a constant input is applied to the motor, it reaches a steady velocity. Since position is the integral of velocity, a constant velocity results in a linearly increasing position — a ramp. The slope of this ramp is proportional to the steady-state velocity, and the constant of proportionality is the integrator gain a. Therefore, a was calculated by dividing the slope of the position ramp by the corresponding velocity.

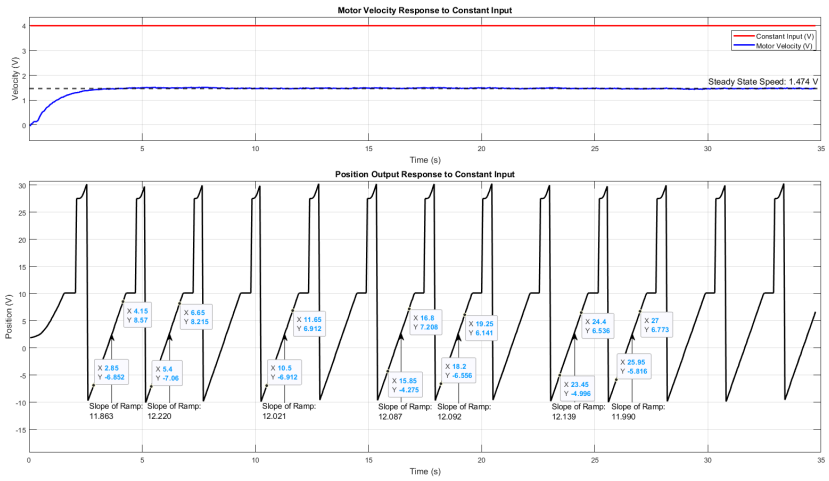

Figure 5: Ramp response of position output used to calculate integrator gain $a = 8.181$

6. Simulink Model

The full second order plant model used for simulation combined the two components:

$$P(w) = \frac{A \cdot a}{w(Tw + 1)}$$

This model was implemented in Simulink and used to simulate system behaviour under varying parameter conditions.

7. Parameter Summary

Table 2: Estimated Plant Parameters Under Different Physical Conditions

Case	**Gain A**	**Time Constant T (s)**	**Integrator Gain a**
Nominal	1.384	0.85	8.181
With Brake	0.437	0.25	8.181
With Mass	1.502	7.55	8.181

8. Frequency Response Validation

To validate the velocity model in the frequency domain, the measured gain and phase of a sinusoid of 1.18 rad / s was compared to the model. The results — approximately -1.22 dB and $-43.95°$ — matched the

behaviour of a first-order lag well.

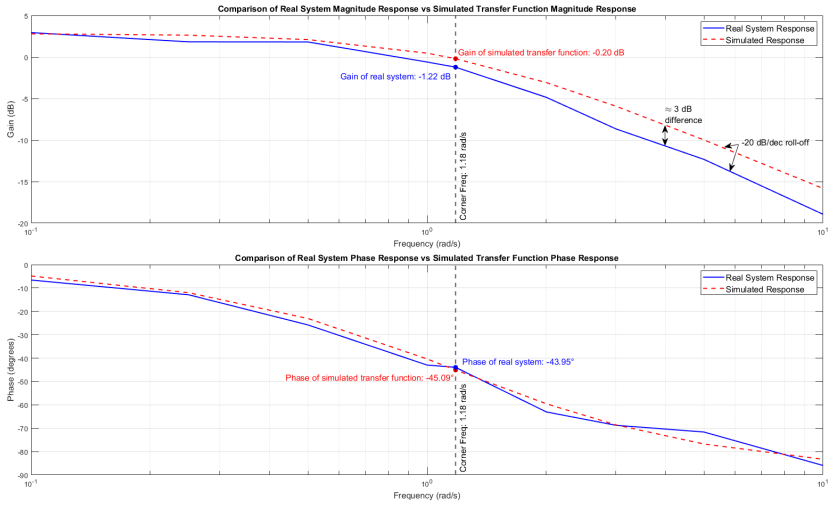

Figure 6: Bode plot of nominal plant showing expected 20 dB/decade roll-off and 45° phase shift

9. Time-Domain Validation

The model's step response was also compared to measured data. The simulated and experimental results matched well in terms of rise time, gain, and time constant.

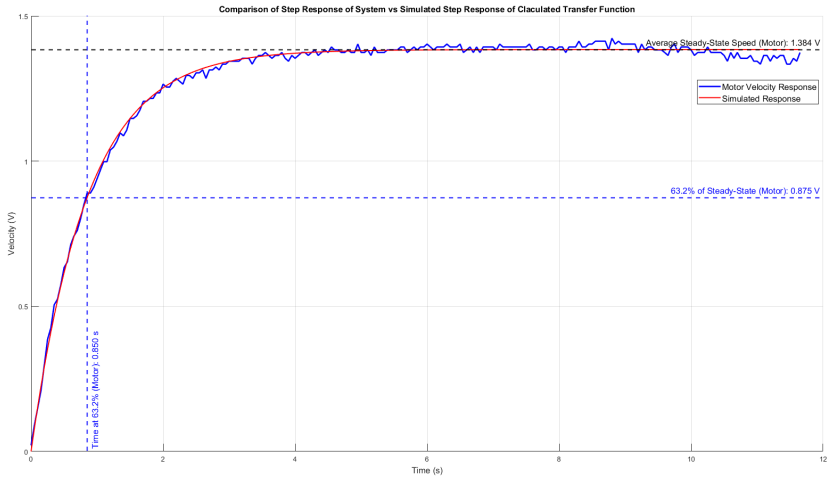

Figure 7: Measured vs simulated step response under nominal conditions

To verify the accuracy of the integrator model, the measured position ramp was compared to the simulated response of the transfer function $P_1(w) = \frac{a}{w}$ using the estimated gain. A constant velocity input was applied in both cases, and the resulting position outputs were plotted over time. The aim was to confirm that the modelled integrator produces the same slope as the real system.

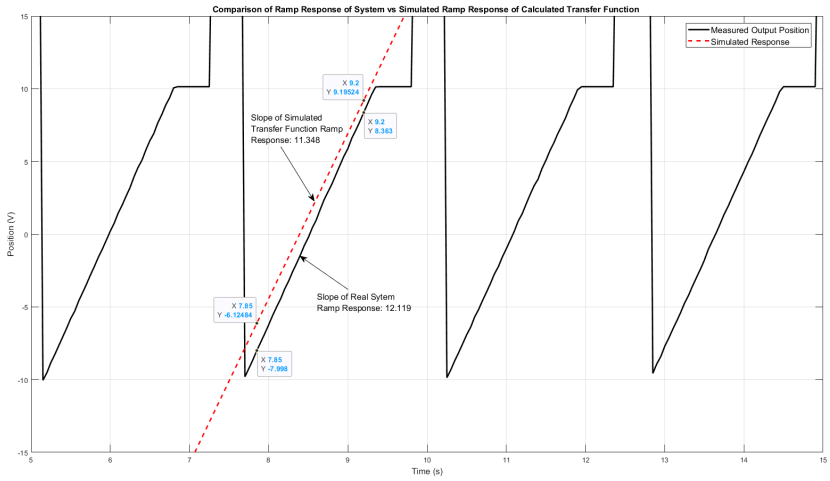

Figure 8: Comparison of measured position ramp and simulated response using the modelled integrator $P_1(w) = \frac{a}{w}$. The close match in slope validates the estimated integrator gain $a = 8.181$.

10. Model Uncertainty Bound

From the data, the gain and time constant varied across different test conditions:

$$A \in [0.437,\ 1.502], \quad T \in [0.25,\ 7.55]$$

These bounds were used in the controller design phase to ensure robustness across the full operating envelope.

0.3 Digital Control Design

1. Control Architecture

The control system uses a cascaded structure:

- A fast inner loop controls motor speed using a proportional controller
- A slower outer loop controls position using a PI controller

This separation allows for simpler controller tuning and better overall performance.

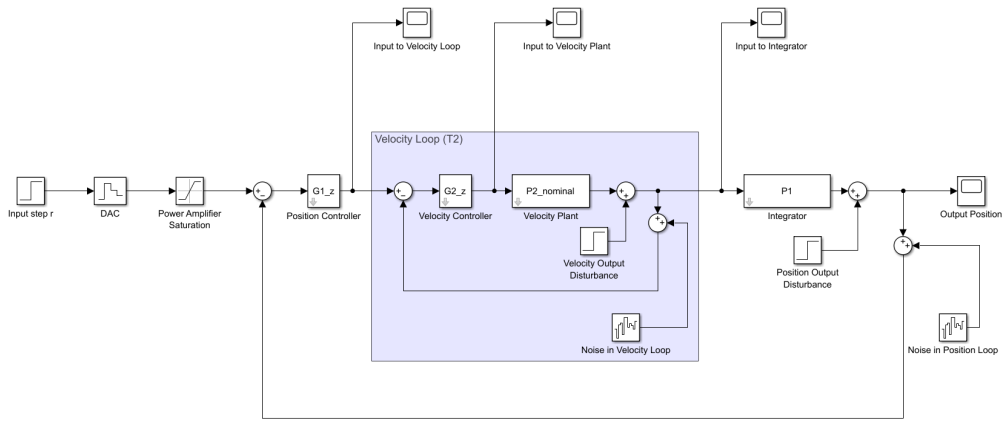

Figure 9: Cascaded digital control structure implemented in Simulink

2. Velocity Loop Design

The velocity loop uses a proportional controller $G_2(w) = K_2$, applied to a first-order plant. The resulting closed-loop transfer function is:

$$T_2(w) = \frac{K_2 A}{\tau w + 1 + K_2 A}$$

This is itself a first-order system, with a single pole at:

$$w = -\frac{1 + K_2 A}{\tau}$$

As K_2 increases, the pole moves further left, improving the speed of the response. The settling time for a first-order system is given by:

$$t_s = 4 \cdot \tau_{\text{cl}} = \frac{4\tau}{1 + K_2 A}$$

To meet the required $t_s < 1\,\text{second}$, the closed-loop pole must satisfy:

$$\frac{4\tau}{1 + K_2 A} < 1 \quad \Rightarrow \quad K_2 > \frac{4\tau - 1}{A}$$

For the nominal parameters ($\tau = 0.85$, $A = 1.384$), this gives:

$$K_2 > \frac{4 \cdot 0.85 - 1}{1.384} \approx 1.84$$

Both tested values — $K_2 = 10$ and $K_2 = 20$ — satisfy this comfortably, but $K_2 = 20$ results in a much faster response and higher phase margin, as seen in the Nichols plot. This made it the preferred choice for the final controller.

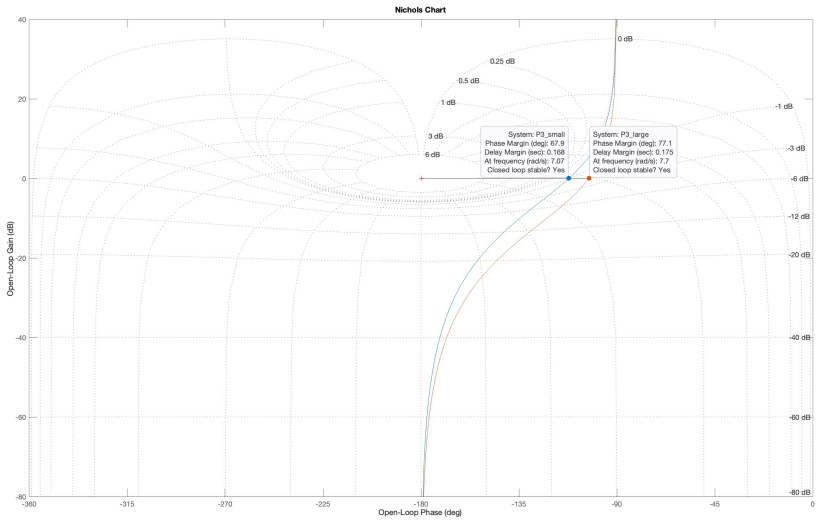

Figure 10: Nichols chart showing improved phase margin for $K_2 = 20$

3. Position Loop Design

The outer loop uses a PI controller of the form:

$$G_1(w) = \frac{w/\alpha + 1}{w}$$

This form adds a zero to improve phase margin while maintaining zero steady-state error due to the integrator.

Damping Specification

The phase margin directly affects the damping ratio and overshoot of the closed-loop step response. To improve robustness, a target overshoot of 10% was selected — better than the 20% specification limit. The damping ratio ζ corresponding to 10% overshoot is:

$$\zeta = \frac{\ln(0.1)}{\sqrt{\pi^2 + (\ln(0.1))^2}} \approx 0.591$$

From EEE3094S, the relationship between damping ratio and phase margin (in degrees) for a second-order system is approximately:

$$\zeta \approx \frac{ACL}{100 \cdot \phi_m}$$

Since the closed-loop gain $ACL = 1$ due to the integrator in the position loop, the required phase margin is:

$$\phi_m = 0.591 \cdot 100 = 59.1^\circ \approx 60^\circ$$

Zero Placement and Sampling Phase Compensation

To achieve this, a phase lead of 60° was needed at the crossover frequency. However, sampling also introduces phase lag at higher frequencies, so this had to be considered. At $\omega = 10\,\text{rad/s}$, the phase lag due to the ZOH was estimated as:

$$\phi_{\text{sampling}} = \tan^{-1}\left(\frac{\omega T}{2}\right) = \tan^{-1}(0.25) \approx 14.04^\circ$$

To compensate for this, the total required phase lead was:

$$\phi_{\text{tot}} = \phi_m + \phi_{\text{sampling}} = 60^\circ + 14^\circ = 74^\circ$$

Using this, the location of the zero was calculated based on:

$$\tan(\phi_{\text{tot}}) = \frac{\omega}{\alpha} \quad \Rightarrow \quad \alpha = \frac{\omega}{\tan(74^\circ)} = \frac{10}{3.49} \approx 2.86$$

For simplicity, the zero was placed at $\alpha = 2.8\,\text{rad/s}$, ensuring enough phase lead to meet stability and performance targets even after discretisation.

Gain of PI Controller

The Nichols chart for the position loop with the integrator and zero is shown in Figure 11. From the plot, we observe that to maximise the phase margin of the nominal plant (labelled 3), the gain must be increased so that the nominal point at approximately -10.7 dB aligns with the gain crossover point. This corresponds to a linear gain of:

$$k = \frac{10^{10.7/20}}{1} \approx 3.6$$

However, this same gain reduces the phase margin of the worst-case plant with added mass (labelled 2) to around 9°, which is insufficient when accounting for additional phase lag due to sampling.

To address this, we increased the phase lead by placing the zero closer to the origin. The new zero was set at $\alpha = 2.3$, as shown in Figure 12. With the new zero, a gain of approximately 9.5 dB was needed to align the nominal curve with the crossover. This corresponds to a linear gain of:

$$k = 10^{9.5/20} \approx 3$$

At this gain, the worst-case plant retains a phase margin of around 14°, which, while low, is sufficient for stabilisation.

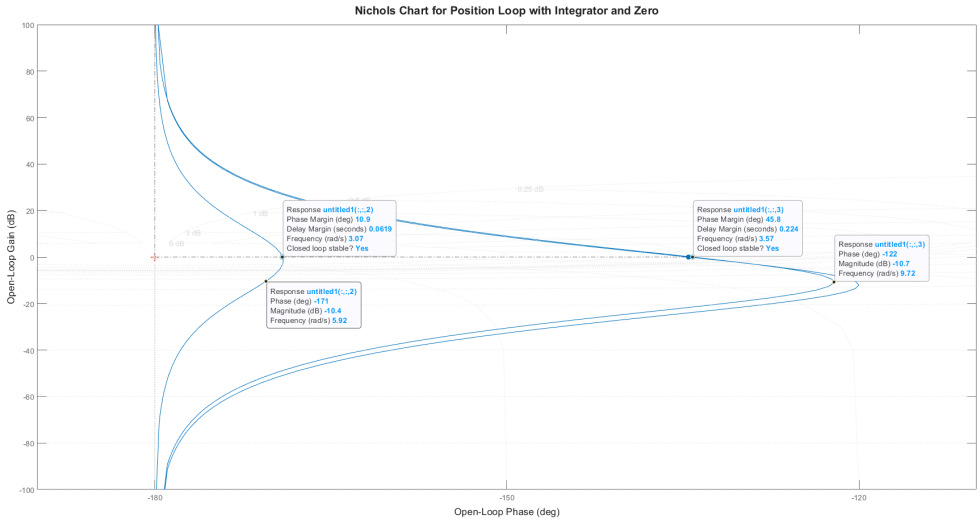

Figure 11: Nichols chart of position loop with integrator and original zero for all plant cases.

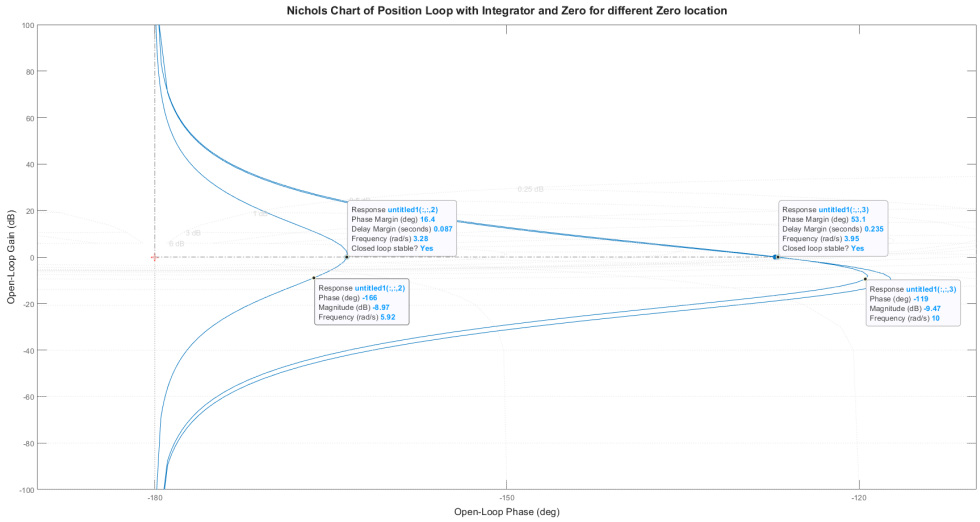

Figure 12: Nichols chart of position loop with integrator and relocated zero at $\alpha = 2.3$.

Ultimately, to meet the time-domain performance requirements — specifically the settling time of under 1 second — the gain was increased slightly to $k = 4$ during simulation.

The Nichols chart of the position loop with the full PI controller (i.e., including both the integrator and the zero with gain $k = 4$) is shown below in Figure 13.

From the chart, the nominal plant achieves a phase margin of approximately 58.9°, from which the sampling-induced lag must be subtracted. This reduced margin is still sufficient to meet the damping requirement.

For the worst-case plant with added mass, the phase margin is approximately 12° before accounting for

sampling lag. This results in a marginally stable but acceptable system. In a more demanding application, a higher-order controller might be required to boost phase margin and robustness.

However, for the purposes of this laboratory, the only requirement is that the controller remains stable across all plant variations — a condition that is currently satisfied.

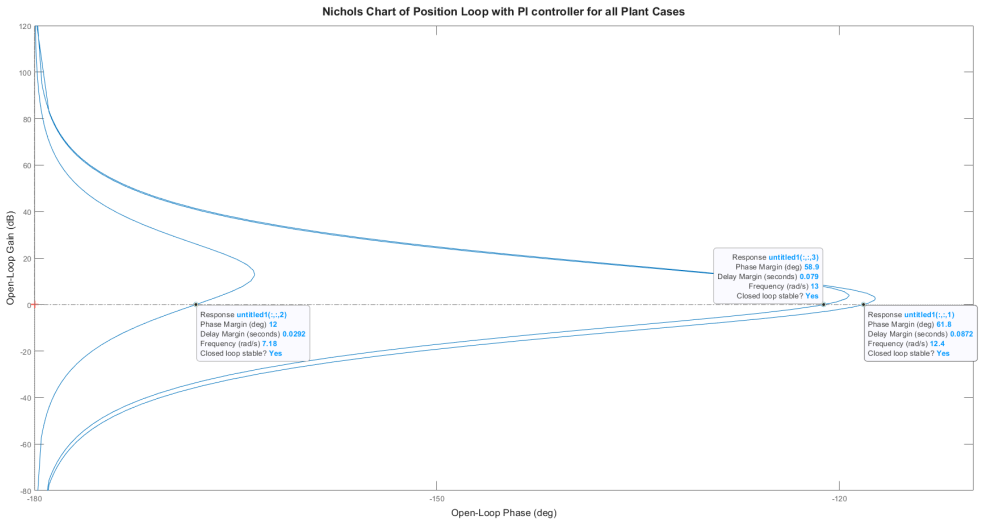

Figure 13: Nichols chart of position loop with final PI controller and all plant cases.

4. Digital Implementation

The design was carried out in the w-domain, then converted to the z-domain using the Tustin (bilinear) method:

```
Gz = c2d(Gw, 0.05, 'tustin');
```

The additional phase lag introduced by the ZOH was estimated and compensated for during the design phase.

5. Final Controller Structure

Velocity Loop:

$$G_2(w) = 20$$

Position Loop:

$$G_1(w) = \frac{\frac{w}{2.8} + 1}{w}$$

Both controllers were implemented in Simulink, where they were tested in simulation and later verified in the lab.

0.4 Simulation and Experimental Validation

1. Simulation Setup

After designing the continuous-time controllers, they were discretised using the Tustin method and implemented in Simulink for full closed-loop simulation. The simulated system included:

- The complete plant model with identified parameters (A, T, a)
- The cascaded digital controllers (inner proportional, outer PI) - as seen in Figure 9
- Step and disturbance inputs

The system was evaluated against the performance specifications — all of which match the assessment criteria used during the controller demonstration.

2. Digital Controller Implementation

After designing the position controller in the w-domain, it was discretised using the Tustin method with a sampling time of $T = 0.05\,\text{s}$. This gave a transfer function $G(z)$ in the z-domain, which was then converted into a time-domain difference equation suitable for real-time implementation.

The general form of the discrete PI controller is:

$$G(z) = \frac{b_0 + b_1 z^{-1}}{1 - a_1 z^{-1}}$$

This corresponds to the time-domain control law:

$$u[k] = a_1 u[k-1] + b_0 e[k] + b_1 e[k-1]$$

Where:

- $u[k]$ is the control signal at time step k
- $e[k]$ is the current error: $e[k] = r[k] - y[k]$
- a_1, b_0, b_1 are coefficients obtained from the discretised controller and are -1, 1.8391, and -1.6391 respectively.

These coefficients correspond to the discretised form of the final PI controller with $k = 4$ and $\alpha = 2.3$, converted using Tustin's method.

These coefficients were extracted directly from MATLAB using the 'tfdata' function:

```
[b, a] = tfdata(Gz, 'v');
b0 = b(1); b1 = b(2);
a1 = -a(2); % note: negative because denominator is (1 - a1*z^-1)
```

This control law was implemented in the lab on the digital platform, updating the output $u[k]$ every 0.05 seconds using the most recent error and past values. The resulting controller was able to drive the system accurately and meet the performance targets in real-time.

3. Assessment Criteria and Results

Settling Time Simulated and measured responses both showed that the system reached steady state within **1 second**.

Set Point Tracking The controller achieved **zero steady-state error** to step inputs. The position output consistently converged to the reference with no visible bias.

Overshoot In both simulation and lab results, overshoot remained **well within 20%**. In most cases, the overshoot was closer to 10%, showing good damping due to the phase margin added by the PI controller.

Disturbance Rejection Disturbance rejection was tested by introducing a brief load or tap to the output. The system returned to the setpoint in less than **1 second**, both in simulation and experimentally.

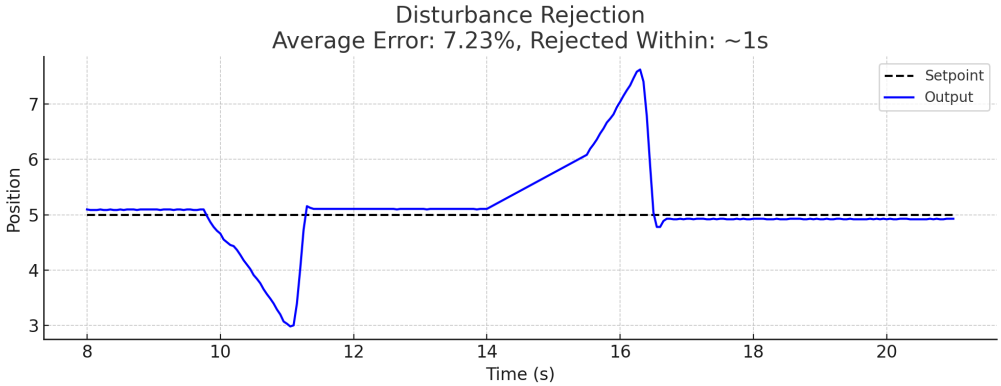

Figure 14: Measured output showing recovery from disturbance in under 1 second

Robustness to Plant Changes The controller remained **stable under plant uncertainty**. Tests with the added brake and additional mass showed no instability or oscillations. The output tracked the setpoint more slowly in these cases — as expected — but with no loss of control.

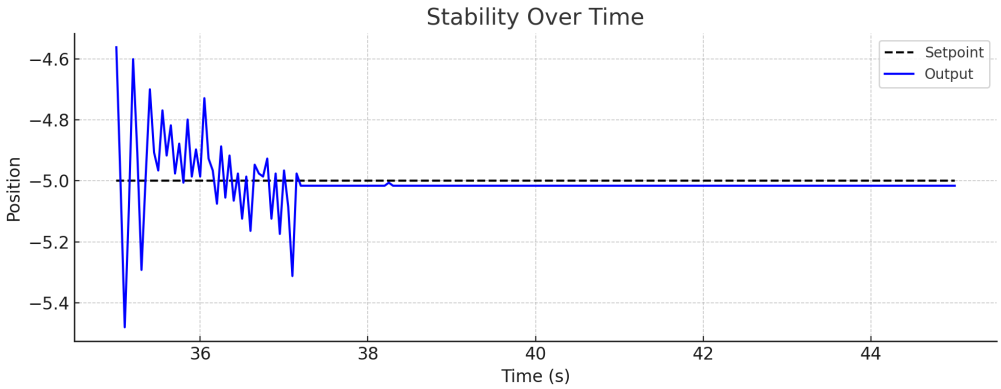

Figure 15: Measured output showing stability over time

4. Final Comparison: Simulation vs Lab Performance

Figures 16 and 17 show the system response to a position step in both Simulink and the real system. The similarity confirms that the model and controller design were accurate.

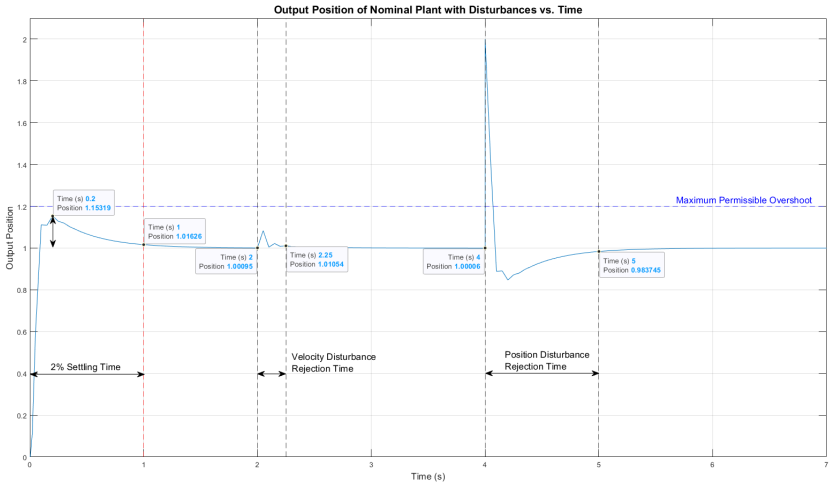

Figure 16: Step Response Output Position of Nominal Plant with Velocity and Position Output Disturbances Added

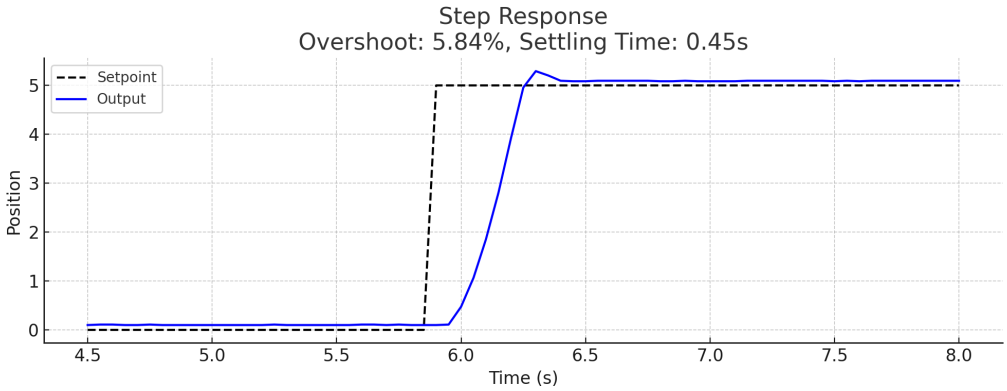

Figure 17: Measured step response in laboratory implementation

5. Summary of Performance vs Specification

Table 3: Controller performance vs marking criteria

Criterion	**Achieved Result**
Settling Time	Within 1 second
Set Point Tracking	Zero steady-state error
Overshoot	$< 20\%$
Disturbance Rejection	Recovery < 1 second
Stability under Changes	Stable in all cases

0.5 Conclusions

This project brought together the essential steps of real-world control system design — from modelling a physical plant to designing and implementing a digital controller that performs reliably under varying conditions.

Beginning with system identification, the motor's behaviour was characterised through step and ramp input

tests. The resulting model captured the system's dynamics effectively, even under altered conditions such as added mass or braking. Based on this model, a cascaded digital controller was designed using standard control techniques and then discretised for real-time implementation.

Simulations and laboratory tests confirmed that the controller met all critical performance criteria: fast settling time, low overshoot, zero steady-state error, and strong disturbance rejection. More importantly, it maintained stability across all tested plant variations, demonstrating the robustness of the design.

This project provided a valuable opportunity to apply engineering theory in a practical setting. Concepts such as transfer functions, phase margins, and difference equations were directly used to build a controller that functioned successfully in hardware. It also reinforced the importance of testing, iteration, and sound engineering judgment when working with physical systems.

Ultimately, this wasn't just an exercise in meeting performance specifications — it was about designing something that works, understanding why it works, and being able to communicate and justify each step of the process. That is the essence of Graduate Attribute 2.

Bibliography

[1] Group 2, *Servo Design Report*, EEE4118F, University of Cape Town, 2025.

[2] Group 2, *System Identification Report*, EEE4118F, University of Cape Town, 2025.